

UCLA

UCLA Previously Published Works

Title

Adipose-Derived Mesenchymal Stromal Cells Persist in Tissue-Engineered Vocal Fold Replacement in Rabbits

Permalink

<https://escholarship.org/uc/item/4cq6621g>

Journal

Annals of Otology Rhinology & Laryngology, 127(12)

ISSN

0003-4894

Authors

Goel, Alexander N
Gowda, Bhavani S
Veena, Mysore S
[et al.](#)

Publication Date

2018-12-01

DOI

10.1177/0003489418806008

Peer reviewed

Annals of Otolaryngology, Rhinology & Laryngology

Adipose-Derived Mesenchymal Stromal Cells Persist in Tissue-Engineered Vocal Fold Replacement in Rabbits

Journal:	<i>Annals of Otolaryngology, Rhinology & Laryngology</i>
Manuscript ID	AOR-18-0470.R1
Manuscript Type:	Original Article
Keywords:	Tissue regeneration < Miscellaneous, tissue stem cell < Miscellaneous, Regenerative Medicine < Miscellaneous, vocal fold histology < Laryngology < Otolaryngology, Dysphonia < Miscellaneous
Abstract:	<p>Objectives Cell therapies using mesenchymal stromal cells (MSCs) have been proposed as a promising new tool for the treatment of vocal fold scarring. However, the mechanisms by which MSC promote healing as well as their duration of survival within the host vocal fold have yet to be defined. The aim of this work was to assess the persistence of embedded MSCs within a tissue-engineered vocal fold mucosal replacement in a rabbit model of vocal fold injury.</p> <p>Methods Male rabbit adipose-derived mesenchymal stromal cells (ASC) were embedded within a three-dimensional fibrin gel, forming the cell-based outer vocal fold replacement (COVR). Four female rabbits underwent unilateral resection of vocal fold epithelium and lamina propria and reconstruction with COVR implantation. Polymerase chain reaction and fluorescent in situ hybridization for the sex-determining region of the Y chromosome (SRY-II) in the sex-mismatched donor-recipient pairs sought persistent cells after 4 weeks.</p> <p>Results A subset of implanted male cells was detected in the implant site at 4 weeks. Many SRY-II negative cells were also detected at the implant site, presumably representing native female cells that migrated to the area. No SRY-II signal was detected in contralateral control vocal folds.</p> <p>Conclusions The emergent tissue after implantation of a tissue-engineered outer vocal fold replacement is derived both from initially embedded adipose-derived stromal cells and infiltrating native cells. Our results suggest this tissue-engineering approach can provide a well-integrated tissue graft with prolonged cell activity for repair of severe vocal fold scars.</p>

1
2
3
4
5
6
7
8
9
10
11
12
13
14
15
16
17
18
19
20
21
22
23
24
25
26
27
28
29
30
31
32
33
34
35
36
37
38
39
40
41
42
43
44
45
46
47
48
49
50
51
52
53
54
55
56
57
58
59
60

SCHOLARONE™
Manuscripts

For Peer Review

1
2
3 1 TITLE: Adipose-Derived Mesenchymal Stromal Cells Persist in Tissue-Engineered Vocal Fold
4 2 Replacement in Rabbits
5 3

6 4 RUNNING TITLE: Cell Persistence In Vocal Fold Replacement
7 5

8 6 AUTHORS:

9 7 Alexander N. Goel, BA^a

10 8 Bhavani S. Gowda, PhD^a

11 9 Mysore S. Veena, PhD^b

12 10 Travis L. Shiba, MD^a

13 11 Jennifer L. Long, MD, PhD^{a,b,*}
14 12

15 13 ^aDepartment of Head and Neck Surgery, David Geffen School of Medicine at University of
16 14 California, Los Angeles, Los Angeles, CA

17 15 ^bResearch Service, Greater Los Angeles Veterans Affairs Hospital System, Los Angeles, CA
18 16

19 17 FINANCIAL SUPPORT: This material is based upon work supported by the Department of
20 18 Veteran Affairs, Veterans Health Administration, Office of Research and Development,
21 19 Biomedical Laboratory Research and Development (Jennifer Long), VA Career Development
22 20 Award IK2BX001944 (Jennifer Long); American Academy of Otolaryngology-Head and Neck
23 21 Surgery Foundation Resident Research Grant (Travis Shiba); Dean's Leadership in Health and
24 22 Science Scholarship at David Geffen School of Medicine (Alexander Goel).
25 23

26 24 CONFLICT OF INTEREST: None
27 25

28 26 FINANCIAL DISCLOSURES: None
29 27

30 28 STATUS: New submission. This work has not been previously published in any language
31 29 anywhere and is not under simultaneous consideration or in press by another journal
32 30

33 31 *CORRESPONDING AUTHOR:

34 32 Dr. Jennifer L. Long

35 33 Email: Jennifer.Long2@va.gov
36 34

37 35 David Geffen School of Medicine at UCLA

38 36 10833 Le Conte Ave

39 37 Los Angeles, Ca 90095

40 38 Ph: 310-825-4949

41 39 Fx: 310-206-7384
42 40

43 41 Research Service

44 42 Greater Los Angeles VAHS

45 43 11301 Wilshire Blvd

46 44 Los Angeles, CA 90073
47 45
48 46
49
50
51
52
53
54
55
56
57
58
59
60

1
2
3 **47 ABSTRACT**
4

5 **48 Objectives**
6

7
8 **49** Cell therapies using mesenchymal stromal cells (MSCs) have been proposed as a promising new
9
10 **50** tool for the treatment of vocal fold scarring. However, the mechanisms by which MSC promote
11
12 **51** healing as well as their duration of survival within the host vocal fold have yet to be defined. The
13
14 **52** aim of this work was to assess the persistence of embedded MSCs within a tissue-engineered
15
16 **53** vocal fold mucosal replacement in a rabbit model of vocal fold injury.
17
18

19 **54**
20
21 **55 Methods**
22

23
24 **56** Male rabbit adipose-derived mesenchymal stromal cells (ASC) were embedded within a three-
25
26 **57** dimensional fibrin gel, forming the cell-based outer vocal fold replacement (COVR). Four
27
28 **58** female rabbits underwent unilateral resection of vocal fold epithelium and lamina propria and
29
30 **59** reconstruction with COVR implantation. Polymerase chain reaction and fluorescent in situ
31
32 **60** hybridization for the sex-determining region of the Y chromosome (SRY-II) in the sex-
33
34 **61** mismatched donor-recipient pairs sought persistent cells after 4 weeks.
35
36
37
38
39

40 **62**
41
42 **63 Results**
43

44
45 **64** A subset of implanted male cells was detected in the implant site at 4 weeks. Many SRY-II
46
47 **65** negative cells were also detected at the implant site, presumably representing native female cells
48
49 **66** that migrated to the area. No SRY-II signal was detected in contralateral control vocal folds.
50
51

52 **67**
53
54 **68 Conclusions**
55
56
57
58
59
60

1
2
3 69 The emergent tissue after implantation of a tissue-engineered outer vocal fold replacement is
4
5 70 derived both from initially embedded adipose-derived stromal cells and infiltrating native cells.
6
7
8 71 Our results suggest this tissue-engineering approach can provide a well-integrated tissue graft
9
10 72 with prolonged cell activity for repair of severe vocal fold scars.
11

12 73

13
14 74 **KEYWORDS:** Adipose-derived stromal cell; tissue engineering; vocal fold scarring; vocal fold
15
16
17 75 replacement
18

19 76

For Peer Review

77 INTRODUCTION

78 Vocal fold scarring, which can be caused by inflammation, radiation, trauma, or surgery, is a
79 disabling voice disorder. Scar tissue alters the extracellular matrix (ECM) of the vocal fold,
80 making it stiff and inelastic, leading to altered voice quality. The composition and organization
81 of the ECM establish the vocal fold's biomechanical properties which in turn determine voice
82 quality. Thus, treatment of the voice disturbance requires restoration of the unique microstructure
83 of the ECM.

84
85 Cell-based approaches have received recent attention as potential therapies for vocal fold
86 scarring. Among various cell types, mesenchymal stromal cells (MSCs) are particularly
87 attractive given their ease of expansion in culture and extensive safety profile in humans.^{1,2}
88 MSCs can be administered alone or combined with a scaffold. Scaffolds provide an instructive
89 microenvironment that may enhance stem cell survival at the site of injury. We previously
90 showed that adipose-derived mesenchymal stromal cells (ASCs) embedded within a three-
91 dimensional fibrin gel scaffold improve vocal fold histology and vibration in rabbits.^{3,4}

92
93 Although MSC have been proposed for vocal fold scarring, the therapeutic mechanisms by
94 which MSC promote healing have yet to be defined. Reasons for benefit may include direct
95 replacement of damaged resident cells, release of immunomodulatory or trophic factors, or a
96 combination thereof. It is known that MSC secrete several anti-fibrotic and prosurvival factors
97 that likely play a role,⁵⁻⁷ but some evidence for differentiation and engraftment has also been
98 reported.⁸ The identification of MSC's powerful paracrine actions in other tissues has de-
99 emphasized long-term cell engraftment as a therapeutic requirement.⁹⁻¹¹ Nonetheless, implanted

1
2
3 100 cells must survive for some unknown duration to produce any paracrine effect. For vocal fold
4
5 101 replacement, in which organized ECM remodeling is the therapeutic action, implanted cell
6
7 102 influence should continue until remodeling is stabilized.
8
9
10 103
11
12 104 Understanding the fate of transplanted stem cells requires reliable techniques for identifying cells
13
14 105 after implantation. Traditional methods using stem cells labeled with transgenic constructs (e.g.
15
16 106 green fluorescent protein) or membrane dyes (e.g. CM-DiI) have been used in the vocal fold with
17
18 107 widely varying findings regarding the timeline of cell survival.¹²⁻¹⁴ These methods are limited by
19
20 108 loss of gene expression in unstable transfections and reduction in the concentration of membrane
21
22 109 dye through cell divisions.^{15,16} An alternative approach implants sex-mismatched ASCs and
23
24 110 seeks signal for Y chromosome DNA.¹⁷ Such an approach capitalizing on donor-specific
25
26 111 antigens may overcome some of the limitations of cell labeling.¹⁷
27
28
29
30
31
32

33 113 The aim of the present study is to assess the engraftment of ASCs within the female rabbit vocal
34
35 114 fold implants that were previously reported.[3,4] Cell-based Outer Vocal fold Replacements
36
37 115 (COVR) were formed with male rabbit ASC in three-dimensional fibrin gel scaffolds. COVRs
38
39 116 were implanted in four female rabbits after removing the native vocal fold epithelium and lamina
40
41 117 propria. Excised larynx phonation and histology results at 4 weeks were previously described.
42
43 118 This study uses Y chromosome DNA to identify persistent donor cells four weeks after
44
45 119 implantation, and TUNEL labeling to identify apoptotic cells.
46
47
48
49
50

120

121 **METHODS**

122 **In Vitro Development of Cell-Based Outer Vocal Fold Replacement**

1
2
3 123 Rabbit adipose-derived multipotent stromal cells (rASCs) were isolated from male rabbits and
4
5 124 tissue-engineered constructs were created as previously described (Figure 1A).^{1,18,19} Briefly,
6
7
8 125 rASCs were harvested from inguinal fat by collagenase digestion and expanded in culture. Cell
9
10 126 multipotency was confirmed by differentiation to osteogenic and adipogenic phenotypes.¹⁸
11
12 127 Rabbit fibrinogen was mixed with bovine thrombin and rASC cell suspension to form fibrin gels
13
14 128 with embedded ASC within 12mm Transwell culture inserts. The tissue constructs were cultured
15
16
17 129 with an air interface and supplied culture medium through the insert base. Medium contained
18
19 130 10% fetal bovine serum and 100 ng/mL of epidermal growth factor. After 2 weeks, the cell-
20
21 131 based outer vocal fold replacements (COVR) were harvested for implantation or baseline
22
23 132 histology. Histologic stains included standard hematoxylin and eosin (H&E), Masson's
24
25 133 trichrome to stain collagen fibers blue, and phosphotungstic acid hematoxylin (PTAH) to stain
26
27 134 fibrin fibers blue. The mature COVR *in vitro* demonstrated homogeneous fibrin fibers, without
28
29
30
31 135 detectable collagen.

32
33 136

35 137 **COVR Implant Surgery**

36
37 138 The **local** Institutional Animal Care and Use Committee approved this study **which was**
38
39 **conducted in accordance with all local and federal guidelines.** Four female New Zealand white
40
41 139 rabbits, weighing 3 to 3.5 kg, underwent survival surgery for outer vocal fold mucosa removal
42
43 140 and implantation with COVR which was described previously.³ Briefly, rabbits were
44
45 141 anesthetized, and the larynx exposed through a neck incision. After laryngofissure, the entire
46
47 142 membranous cover layer was resected from the left inferior vocal fold. Immediately following
48
49 143 resection, a mature COVR containing male rASC was placed to fill the defect and secured with
50
51 144 sutures and fibrin glue. All right vocal folds remained as untreated controls. The laryngofissure,
52
53
54 145

1
2
3 146 tracheotomy, and neck were closed and the animals recovered. Intramuscular dexamethasone,
4
5 147 analgesics, and antibiotics were administered for three days to prevent laryngeal edema, pain,
6
7
8 148 and infection. All four animals recovered without complication or apparent distress, maintained
9
10 149 oral diet, and gained weight. After 4 weeks, animals were euthanized and larynges harvested.
11
12 150 The 4-week time point was chosen for best comparison with previous work in this laboratory and
13
14
15 151 because it lies within the range of other studies assessing MSC persistence.^{3,4,8,13,20} All four
16
17 152 larynges produced phonation in an excised larynx setup, the same day as harvest as described
18
19 153 previously.³ Larynges were then formalin-fixed and paraffin-embedded (FFPE) for sectioning
20
21 154 and DNA extraction.
22
23
24 155

26 156 **PCR Amplification of Rabbit Y Chromosome DNA**

27
28 157 Genomic DNA from male New Zealand white rabbit thymuses was isolated and purified using
29
30
31 158 the Qiagen genomic DNA kit (Germantown, MD). Primers were constructed for the second sex-
32
33 159 determining region of the Y chromosome (SRY-II) of the European brown hare.²¹ The isolated
34
35 160 DNA was amplified by PCR using the SRY-II primers with AmpliTaq Gold™ 360 Master Mix
36
37 161 (Applied Biosystems, Foster City, CA) under the following conditions: 95°C for 2 minutes
38
39
40 162 followed by 35 cycles of 95°C for 45 seconds, 55°C for 30 seconds, 72°C for 45 seconds with a
41
42 163 final extension at 72°C for 5 minutes. PCR products were run on 1.5% agarose gel and images
43
44
45 164 were captured using G:BOX chemi XRQ (Syngene, Frederick, MD) to confirm expected SRY-II
46
47 165 size of 670 base pairs.
48

49 166

50
51
52 167 After validating the primer sequence with male rabbit DNA, the primers were used to amplify
53
54 168 DNA from rabbit larynx tissues. Implanted female rabbit vocal fold tissues were dissected out of
55
56
57
58
59
60

1
2
3 169 the paraffin blocks, using a scalpel to sharply divide the implanted (left) and control (right) vocal
4
5 170 folds at the anterior commissure (as indicated in Figure 1B). DNA was isolated and purified
6
7
8 171 using the QIAamp DNA FFPE tissue kit (Qiagen, Germantown, MD). PCR amplification
9
10 172 proceeded as above using SRY-II primers. PCR products were separated on 1.5% agarose gel
11
12 173 and imaged.

13
14
15 174

17 175 **Fluorescent In Situ Hybridization (FISH)**

18 176
19 177 DNA was isolated from normal male rabbit thymus, and Y chromosome-specific DNA was then
20
21
22 178 amplified as described above. PCR products were separated on 0.8% agarose gel. The amplified
23
24 179 670 bp SRY-II product was excised from the gel and purified using QIAquick Gel Extraction kit
25
26 180 (Qiagen, Germantown, MD). Purified DNA was labeled with Alexa Fluor 647 dye using Fish
27
28 181 Tag DNA multicolor kit (Molecular Probes, Eugene, OR) following the protocol provided with
29
30
31 182 the kit.

32
33 183

34
35 184 Five-micron FFPE tissue sections of implanted rabbit larynges were used for FISH. Y
36
37 185 chromosome-specific rabbit DNA labeled with Alexa Fluor 647 was used as FISH probe. Tissue
38
39
40 186 sections fixed on glass slides were de-paraffinized in Xylene (with three changes of 5 minutes
41
42 187 each), then gradually rehydrated using 100%, 85%, and 50% ethanol (one minute each) followed
43
44 188 by incubation in 0.2 N HCl for 20 minutes, distilled water for 10 minutes, 2X sodium-saline
45
46 189 citrate for two minutes, 10mM sodium citrate buffer pH 6.0 at 80°C for 30 minutes, 20 ng
47
48
49 190 proteinase K/ml in 10 mM HCl at 37°C for 20 minutes and finally in distilled water for three
50
51 191 minutes. Slides were then dehydrated gradually in 50%, 70%, 85% and 100% ethanol (one
52
53 192 minute each) and air dried for 30 minutes. For the rest of the procedures for pre-hybridization,

1
2
3 193 hybridization, and post-hybridization, washes were carried out as described in the Fish Tag
4
5 194 multicolor kit user guide (Invitrogen, Carlsbad, CA). Slides were coverslipped and imaged with a
6
7
8 195 647 nm fluorescence microscopy filter.
9

10 196

11 12 197 **Apoptosis Assay**

13
14 198 Terminal deoxynucleotidyl transferase dUTP nick-end labeling (TUNEL) assay for apoptotic
15
16
17 199 cells was performed on paraffin-embedded, formalin-fixed slides from implanted rabbit larynges
18
19 200 (Trevigen TACS 2TdT DAB labeling kit, Gaithersburg, MD). The terminal deoxynucleotidyl
20
21 201 transferase (TdT) enzyme incorporated biotin label into fragmented DNA of apoptotic cells.
22
23 202 Positive controls were treated with TACS-Nuclease enzyme to induce DNA strand nicks. Biotin
24
25 203 was detected with diaminobenzidine (DAB) substrate, and nuclei counterstained with methyl
26
27 204 green. Images were taken at 40x.
28
29

30 205

31 32 33 206 **RESULTS**

34 35 207 **Rabbit Y chromosome PCR**

36
37 208 Thymic DNA from normal male New Zealand white rabbits confirmed amplification with the
38
39 209 SRY-II primer sequences, producing a 670 bp PCR product.
40
41

42 210

43
44 211 DNA was isolated from implanted and control rabbit vocal folds, amplified with SRY-II primers,
45
46 212 and separated on agarose. All four implanted vocal folds (with male cells applied to female
47
48 213 larynx) showed an amplified DNA band that corresponded with the 670 bp PCR product from
49
50 214 male thymus. All four contralateral control vocal folds (female larynx without implant) lacked
51
52 215 any amplification with the SRY-II primer (Figure 2A).
53
54
55
56
57
58
59
60

1
2
3 2164
5 217 **Fluorescent In Situ Hybridization (FISH)**

6
7
8 218 In situ hybridization with a tagged SRY-II probe confirmed the findings of PCR. In all four
9
10 219 female larynges, scattered positive (male) cells were detected on the operated side. The area of
11
12 220 implantation also contained many cells negative for the Y-chromosome signal that presumably
13
14 221 represented native female cells that had migrated into the implanted site (Figure 2B). Implanted
15
16 222 ASCs were primarily localized to the lamina propria, with relatively fewer in the epithelial layer
17
18 223 and occasional pockets detected in deep tissue near the thyroarytenoid muscle. No SRY-positive
19
20 224 cells were detected in contralateral control vocal folds.
21
22
23
24 225

25
26 226 **Histological Examination**

27
28 227 Figure 1B shows H&E staining, with implanted left vocal fold appearing similar to unoperated
29
30 228 right vocal fold. Collagen fibers were previously demonstrated in the region of implantation on
31
32 229 Masson's trichrome stain, indicating remodeling of the provisional scaffold.³ Phosphotungstic
33
34 230 acid hematoxylin (PTAH) staining was attempted to determine persistence of the fibrin matrix,
35
36 231 but the non-specific nature of the staining was judged to be inconclusive.
37
38
39
40 232

41
42 233 **Apoptosis assay**

43
44 234 TUNEL labeling for apoptotic cells was negative within the area of COVR implant, consistent
45
46 235 with its negative labeling in contralateral unoperated vocal folds. Positive controls of nuclease
47
48 236 enzyme-treated implant slides did demonstrate positive TUNEL staining, confirming the labeling
49
50 237 technique (Figure 3).
51
52
53
54 238

1
2
3 **239 DISCUSSION**
4

5 240 In this study, we investigated the engraftment of rabbit ASCs within a tissue-engineered implant
6
7 241 in the rabbit vocal fold. To distinguish transplanted cells from native cells, male rASCs were
8
9
10 242 seeded into female hosts to permit DNA analysis for genes on the Y-chromosome. Four weeks
11
12 243 after implantation, scattered male cells were localized within the implant site, along with many
13
14 244 cells that were negative for the fluorescence hybridization signal. This finding suggests that the
15
16 245 emergent tissue derives both from infiltrating native cells and implanted ASCs that were initially
17
18 246 seeded onto the scaffold.
19

20
21 247
22
23 248 Simple injections of mesenchymal stromal cells have prevented scar formation in previous
24
25 249 animal models.^{20,22,23} Postulated mechanisms include secretion of growth factors active in vocal
26
27 250 fold tissue repair, including hepatocyte growth factor (HGF) and fibroblast growth factor 2
28
29 251 (FGF2).^{7,24,25} In addition, Hiwatashi et al reported that MSC treatment led to increased host
30
31 252 expression of hyaluronan synthase, which is thought to maintain viscoelastic function of the
32
33 253 vocal folds.¹² Transient cell activity may be adequate to prevent scarring when the cells are
34
35 254 applied concordant with injury. However, accumulating data have revealed that the survival rate
36
37 255 of cells injected into previously scarred vocal folds is disappointingly low. Svensson et al did not
38
39 256 detect any GFP-positive MSC three months after direct administration in scarred rabbit vocal
40
41 257 folds.²⁶ de Bonnecaze studied an earlier 3-week time point and also were unable to detect GFP-
42
43 258 labeled **cells** after MSC injection.¹³ Survival of transplanted cells is limited by apoptosis, lack of
44
45 259 trophic factors, pathologic conditions, and the inflammatory response.
46
47
48
49
50

51 260
52
53
54
55
56
57
58
59
60

1
2
3 261 Scaffolds, including hyaluronic acid (HA) based hydrogels^{27,28} and atelocollagen,²² have been
4
5 262 used as delivery carriers and led to increased cell survival in a few prior studies. These scaffolds
6
7 263 can be engineered to mimic the native extracellular matrix which may create a microenvironment
8
9 264 more suitable to MSC survival. HA scaffolds have been most widely employed, but are limited
10
11 265 by challenges in preventing HA degradation and clearance in vivo that allows cells to migrate
12
13 266 rapidly away from the site of implantation.²⁹ In the largest pre-clinical trial for vocal fold scar,
14
15 267 Bartlett et al investigated cell engraftment after administration of MSC with and without a
16
17 268 hyaluronic acid gel carrier in rabbits and detected no transplanted cells in either group at 2
18
19 269 weeks.³⁰ In contrast, our study utilized fibrin as the scaffold matrix and detected implanted cells
20
21 270 at 4 weeks in all four female rabbits. Protein-based scaffolds, such as fibrin, may be superior in
22
23 271 promoting cell-to-surface binding compared to polysaccharide-based scaffolds such as HA,
24
25 272 potentially enhancing cell survival.³¹ We hypothesize that the fibrin scaffold provides a
26
27 273 supportive niche which improves cell survival relative to cell injection alone. Whether the
28
29 274 surviving ASCs establish a long-term, stable sub-population residing within the scaffold cannot
30
31 275 be adequately determined by our 4-week study, but this is a question worthy of further
32
33 276 investigation. In this study, host cells did significantly infiltrate the implant, which by 4 weeks
34
35 277 was more host-derived than graft-derived.
36
37
38
39
40
41
42
43

44 279 Characterizing the fate of transplanted cells in regenerative medicine applications depends on
45
46 280 having reliable techniques for cell tracking or detection. To date, methods to identify implanted
47
48 281 stem cells in the vocal fold have primarily relied on transgene construct labeling (e.g. green
49
50 282 fluorescent protein) or membrane dye approaches. These methods are attractive given their ease
51
52 283 of use, but suffer potential limitations in the long-term evaluation of stem cell persistence. The
53
54
55
56
57
58
59
60

1
2
3 284 GFP transgene may become silenced as cells proliferate and differentiate *in vivo*, potentially
4
5 285 masking cell detection.^{15,16,30} Alternatively, lipophilic membrane labels such as carbocyanine
6
7 286 derivatives may be detected even after macrophage ingestion of dead cells, potentially leading to
8
9
10 287 overestimation of surviving cell populations.³² Here, we target sex-specific antigens existing
11
12 288 exclusively in the injected cells by immunofluorescence in a sex-mismatched animal model.
13
14 289 Such a technique may overcome the limitations of cell labeling methods without a significant
15
16 290 increase in complexity or cost and may be a desirable approach for future studies. The limitation
17
18
19 291 of this approach is that it only applies to male cells in female hosts.
20
21 292
22
23 293 Because this methodology of Y-chromosome detection is invalid in the male-male transplant, the
24
25 294 cell persistence in male hosts remains unknown. Inflammatory cell infiltrate did occur in the
26
27 295 female hosts but not in male hosts receiving allogeneic male cells.³ This study transplanted
28
29 296 allogeneic ASCs in the absence of immunosuppression, and the persistence of some implanted
30
31 297 cells after 4 weeks indicates the inflammatory response did not reach the level of complete
32
33 298 transplant rejection. ASCs themselves have significant immunomodulatory activity, which could
34
35 299 assist implanted cells in evading the host immune system.^{33,34} Why the females exhibited greater
36
37 300 leukocytosis is of interest for further investigation. It is conceivable that the female host has
38
39 301 inherently greater immune activity than the males. Or, the greater female response may simply
40
41 302 be due to greater antigen mismatch with male cells. In studies of solid organ transplant in
42
43 303 humans, it has been observed that sex mismatch in donor-recipient pairs, especially cases of male
44
45 304 donor to female recipient, does lead to higher incidence of acute rejection.^{35,36} The mechanism
46
47 305 has been linked to the production of alloantibodies against the male H-Y minor
48
49 306 histocompatibility complex antigen.³⁷ Very limited basic work in cell therapies has explored sex
50
51
52
53
54
55
56
57
58
59
60

1
2
3 307 as a biological variable, which is essential to distinguish these hypotheses in future research.³⁸
4

5 308 For eventual clinical applications, the use of autologous or bank-matched stem cells would be
6

7
8 309 expected to further reduce immune response which could prolong cell survival.
9

10 310

11
12 311 **CONCLUSION**
13

14 312 This study furthers the pre-clinical development of a tissue-engineered outer vocal fold
15

16 313 replacement constructed from adipose-derived stromal cells. A subset of the implanted cells
17

18 314 persisted at least 4 weeks in rabbits, in contrast to other studies with different implant designs.
19

20 315 Our results suggest this tissue-engineering approach can provide a well-integrated tissue graft
21

22 316 with prolonged cell activity for repair of severe vocal fold scars.
23

24
25
26 317
27

28 318
29
30
31
32
33
34
35
36
37
38
39
40
41
42
43
44
45
46
47
48
49
50
51
52
53
54
55
56
57
58
59
60

319 REFERENCES

- 320 1. Zuk P, Zhu M, Mizuno H, et al. Multilineage Cells from Human Adipose Tissue:
321 Implications for Cell-Based Therapies. *Tissue Engineering*. 2001;7(2):211-228.
- 322 2. Pittenger MF, Mackay AM, Beck SC, et al. Multilineage Potential of Adult
323 Human Mesenchymal Stem Cells. *Science*. 1999;284(5411):143-147.
- 324 3. Shiba TL, Hardy J, Luegmair G, Zhang Z, Long JL. Tissue-Engineered Vocal Fold
325 Mucosa Implantation in Rabbits. *Otolaryngol Head Neck Surg*. 2016;154(4):679-688.
- 326 4. Long JL. Repairing the vibratory vocal fold. *Laryngoscope*. 2018;128(1):153-159.
- 327 5. Hirano S, Bless D, Rousseau B, et al. Prevention of Vocal Fold Scarring by Topical
328 Injection of Hepatocyte Growth Factor in a Rabbit Model. *Laryngoscope*.
329 2004;114(3):548-556.
- 330 6. Cheng SL, Zhang SF, Mohan S, et al. Regulation of insulin-like growth factors I and II
331 and their binding proteins in human bone marrow stromal cells by dexamethasone. *J Cell*
332 *Biochem*. 1998;71(3):449-458.
- 333 7. Weimar IS, Voremans C, Bourhis JH, et al. Hepatocyte growth factor/scatter factor
334 (HGF/SF) affects proliferation and migration of myeloid leukemic cells. *Leukemia*.
335 1998;12(8):1195-1203.
- 336 8. Cedervall J, Ahrlund-Richter L, Svensson B, et al. Injection of embryonic stem cells into
337 scarred rabbit vocal folds enhances healing and improves viscoelasticity: short-term
338 results. *Laryngoscope*. 2007;117(11):2075-2081.
- 339 9. Chimenti I, Smith RR, Li TS, et al. Relative roles of direct regeneration versus paracrine
340 effects of human cardiosphere-derived cells transplanted into infarcted mice. *Circ Res*.
341 2010;106(5):971-980.
- 342 10. Li TS, Cheng K, Malliaras K, et al. Direct comparison of different stem cell types and
343 subpopulations reveals superior paracrine potency and myocardial repair efficacy with
344 cardiosphere-derived cells. *J Am Coll Cardiol*. 2012;59(10):942-953.
- 345 11. Furuta T, Miyaki S, Ishitobi H, et al. Mesenchymal Stem Cell-Derived Exosomes
346 Promote Fracture Healing in a Mouse Model. *Stem Cells Transl Med*. 2016;5(12):1620-
347 1630.
- 348 12. Hiwatashi N, Hirano S, Mizuta M, et al. Adipose-derived stem cells versus bone marrow-
349 derived stem cells for vocal fold regeneration. *Laryngoscope*. 2014;124(12):E461-469.
- 350 13. de Bonnecaze G, Chaput B, Woisard V, et al. Adipose stromal cells improve healing of
351 vocal fold scar: Morphological and functional evidences. *Laryngoscope*.
352 2016;126(8):E278-285.
- 353 14. Liang Q, Liu S, Han P, et al. Micronized acellular dermal matrix as an efficient
354 expansion substrate and delivery vehicle of adipose-derived stem cells for vocal fold
355 regeneration. *Laryngoscope*. 2012;122(8):1815-1825.
- 356 15. Brazelton TR, Blau HM. Optimizing Techniques for Tracking Transplanted Stem Cells
357 In Vivo. *Stem Cells*. 2005;23(9):1251-1265.
- 358 16. Toth ZE, Shahar T, Leker R, et al. Sensitive detection of GFP utilizing tyramide signal
359 amplification to overcome gene silencing. *Exp Cell Res*. 2007;313(9):1943-1950.
- 360 17. Terrovitis JV, Smith RR, Marban E. Assessment and optimization of cell engraftment
361 after transplantation into the heart. *Circ Res*. 2010;106(3):479-494.

- 1
2
3 362 18. Shiba T, Hardy J, Long J, Chatzistefanou I. Laryngeal Tissue Engineering Using Rabbit
4 363 Adipose Derived Stem Cells In Fibrin: A Pre-Clinical Model. *Journal of Otolaryngology*
5 364 *Advances*. 2015;1(1):27-39.
- 6 365 19. Long JL, Zuk P, Berke GS, Chhetri DK. Epithelial differentiation of adipose-derived
7 366 stem cells for laryngeal tissue engineering. *Laryngoscope*. 2010;120(1):125-131.
- 8 367 20. Kim YM, Oh SH, Choi JS, et al. Adipose-derived stem cell-containing hyaluronic
9 368 acid/alginate hydrogel improves vocal fold wound healing. *Laryngoscope*.
10 369 2014;124(3):E64-72.
- 11 370 21. Putze M, Nürnberg S, Fickel J. Y-chromosomal markers for the European brown hare
12 371 (*Lepus europaeus*, Pallas 1778). *European Journal of Wildlife Research*. 2007;53(4):257-
13 372 264.
- 14 373 22. Hiwatashi N, Hirano S, Suzuki R, et al. Comparison of ASCs and BMSCs combined with
15 374 atelocollagen for vocal fold scar regeneration. *Laryngoscope*. 2016;126(5):1143-1150.
- 16 375 23. Kanemaru S, Nakamura T, Omori K, et al. Regeneration of the vocal fold using
17 376 autologous mesenchymal stem cells. *Ann Otol Rhinol Laryngol*. 2003;112(11):915-920.
- 18 377 24. Kishimoto Y, Hirano S, Kitani Y, et al. Chronic vocal fold scar restoration with
19 378 hepatocyte growth factor hydrogel. *Laryngoscope*. 2010;120(1):108-113.
- 20 379 25. Suehiro A, Hirano S, Kishimoto Y, Tateya I, Rouzseau B, Ito J. Effects of basic
21 380 fibroblast growth factor on rat vocal fold fibroblasts.
22 381 . *Ann Otol Rhinol Laryngol*. 2010;119(10):690-696.
- 23 382 26. Svensson B, Nagubothu RS, Cedervall J, et al. Injection of human mesenchymal stem
24 383 cells improves healing of scarred vocal folds: analysis using a xenograft model.
25 384 *Laryngoscope*. 2010;120(7):1370-1375.
- 26 385 27. Thibeault SL, Kiemuk SA, Smith ME, Leugers C, Prestwich G. In Vivo Comparison of
27 386 Biomimetic Approaches for Tissue Regeneration of the Scarred Vocal Fold. *Tissue*
28 387 *Engineering: Part A*. 2009;15(7):1481-1487.
- 29 388 28. Xu W, Hu R, Fan E, Han D. Adipose-Derived Mesenchymal Stem Cells in Collagen-
30 389 Hyaluronic Acid Gel Composite Scaffolds for Vocal Fold Regeneration. *Ann Otol Rhinol*
31 390 *Laryngol*. 2011;120(2):123-130.
- 32 391 29. Lim JY, Kim HS, Kim YH, Kim KM, Choi HS. PMMA (polymethylmetacrylate)
33 392 microspheres and stabilized hyaluronic acid as an injection laryngoplasty material for the
34 393 treatment of glottal insufficiency: in vivo canine study. *Eur Arch Otorhinolaryngol*.
35 394 2008;265(3):321-326.
- 36 395 30. Bartlett RS, Guille JT, Chen X, Christensen MB, Wang SF, Thibeault SL. Mesenchymal
37 396 stromal cell injection promotes vocal fold scar repair without long-term engraftment.
38 397 *Cytotherapy*. 2016;18(10):1284-1296.
- 39 398 31. Ahearne M, Kelly DJ. A comparison of fibrin, agarose and gellan gum hydrogels as
40 399 carriers of stem cells and growth factor delivery microspheres for cartilage regeneration.
41 400 *Biomed Mater*. 2013;8(3):035004.
- 42 401 32. Cocco R, Ucker DS. Distinct modes of macrophage recognition for apoptotic and
43 402 necrotic cells are not specified exclusively by phosphatidylserine exposure. *Molecular*
44 403 *Biology of the Cell*. 2001;12(4):919-930.
- 45 404 33. Melief SM, Zwaginga JJ, Fibbe WE, Roelofs H. Adipose tissue-derived multipotent
46 405 stromal cells have a higher immunomodulatory capacity than their bone marrow-derived
47 406 counterparts. *Stem Cells Transl Med*. 2013;2(6):455-463.

- 1
2
3 407 34. Niemeyer P, Kornacker M, Mehlhorn A, et al. Comparison of immunological properties
4 408 of bone marrow stromal cells and adipose tissue-derived stem cells before and after
5 409 osteogenic differentiation in vitro. *Tissue Eng.* 2007;13(1):111-121.
6
7 410 35. Candinas D, Gunson B, Nightingale P, Hubscher S, McMaster P, Neuberger JM. Sex
8 411 mismatch as a risk factor for chronic rejection of liver allografts. *The Lancet.*
9 412 1995;346(8983):1117-1121.
10 413 36. Li Z, Mei S, Xiang J, et al. Influence of donor-recipient sex mismatch on long-term
11 414 survival of pancreatic grafts. *Sci Rep.* 2016;6:29298.
12 415 37. Tan JC, Wadia PP, Coram M, et al. H-Y antibody development associates with acute
13 416 rejection in female patients with male kidney transplants. *Transplantation.*
14 417 2008;86(1):75-81.
15 418 38. Klein SL, Flanagan KL. Sex differences in immune responses. *Nat Rev Immunol.*
16 419 2016;16(10):626-638.
17
18 420
19
20 421

For Peer Review

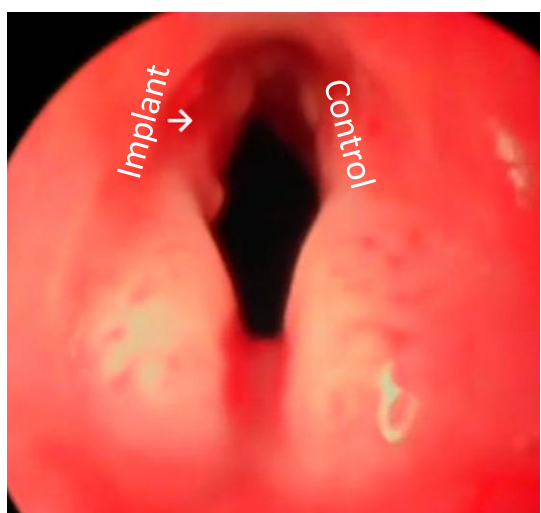
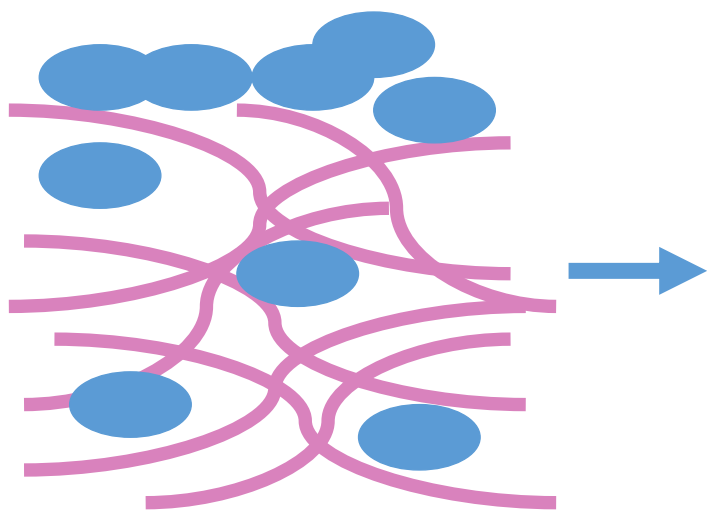
1
2
3 422 **FIGURE LEGENDS**
4

5 423 **Figure 1.** (A) Donor male rASCs were seeded in a COVR that was surgically implanted to
6 female rabbit recipients. (B) Hematoxylin and eosin (H & E) stain of harvested larynx, where left
7 424 vocal fold received COVR implant (L) and right vocal fold served as unoperated control (R).
8 425
9
10 426 10x. (Rabbit 4). Thick black line at the anterior commissure indicates the dividing line for
11
12
13 427 extracting DNA from individual vocal folds.
14
15
16
17 428

18
19 429 **Figure 2.** Presence of implanted cell DNA after 1 month. (A) PCR amplification of SRY-II
20 DNA sequence. "SRY control": normal male rabbit tissue. Lanes are shown for each rabbit's
21 430 implanted vocal fold ("Implant") and contralateral non-implanted vocal fold ("Contra"). (B)
22
23 431 Fluorescent in-situ hybridization for Y chromosome DNA (SRY-II probe, appearing red) in
24
25 432 female rabbit vocal folds 4 weeks after implantation of a COVR seeded with male ASCs. Signal
26
27 433 appears in the operated left vocal folds (L), but not in the contralateral unoperated right vocal
28
29 434 folds (R), suggesting engraftment of implanted ASCs. Nuclei are stained with DAPI (blue).
30
31 435 Rabbit 1 at 4X magnification, Rabbit 2 at 10X magnification.
32
33
34
35 436
36
37
38 437

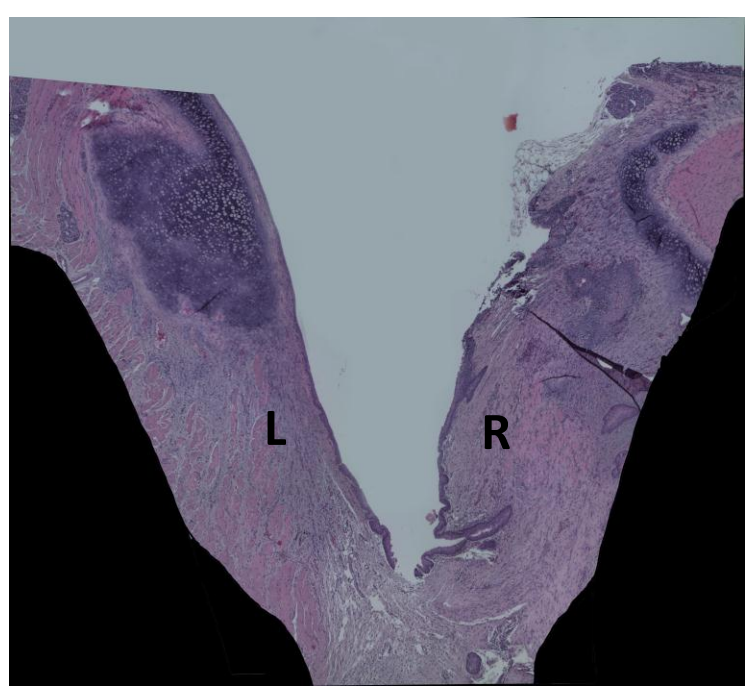
39
40 438 **Figure 3.** TUNEL labeling for apoptotic cells. (A) Positive control for TUNEL staining,
41 enzymatically treated to induce DNA nicks. R4, 40x (B) Harvested left vocal fold (COVR
42 439 implant side) with negative TUNEL staining confirmed that the cells were not undergoing
43
44 440 apoptosis. Rabbit 3, 40x. (C) Harvested right vocal fold (unoperated control) also with negative
45
46 441 TUNEL staining, as expected. Rabbit 3, 40x.
47
48
49 442
50
51
52 443

1
2
3
4
5
6
7
8
9
10
11
12
13
14
15
16
17
18
19
20
21
22
23
24
25
26
27
28
29
30
31
32
33
34
35
36
37
38
39
40
41
42
43
44
45
46
47
48
49
50
51
52
53
54
55
56
57
58
59
60

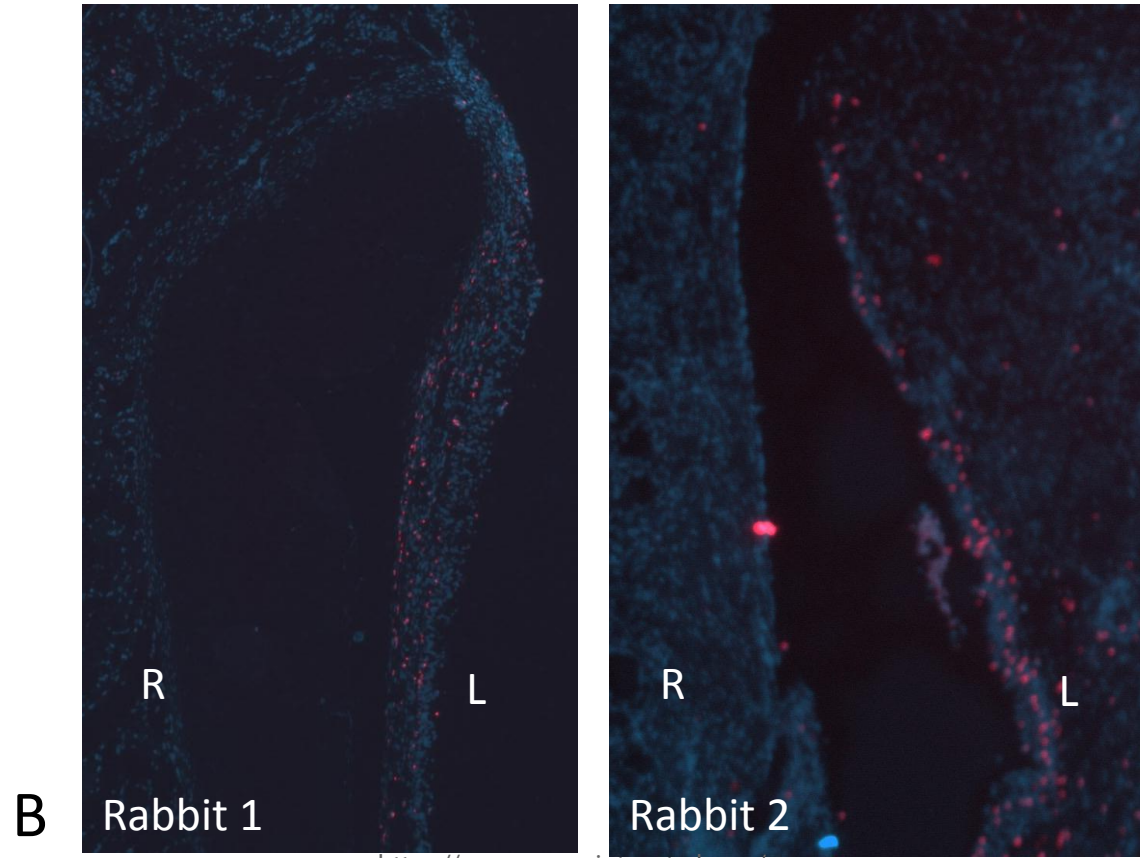
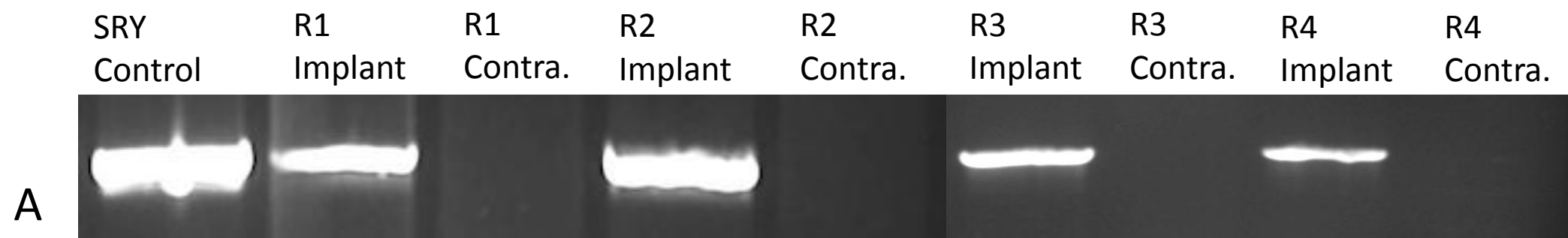


♂ ASC

♀ Rabbit



B



1
2
3
4
5
6
7
8
9
10
11
12
13
14
15
16
17
18
19
20
21
22
23
24
25
26
27
28
29
30
31
32
33
34
35
36
37
38
39
40
41
42
43
44
45
46
47

